A Deep learning framework for seismic facies classification

Harpreet Kaur, Nam Pham, Sergey Fomel, Zhicheng Geng, Luke Decker, Ben Gremillion, Michael Jervis, Ray Abma, and Shuang Gao, The University of Texas at Austin.*

SUMMARY

We propose a deep neural network based framework for seismic facies classification. The proposed framework utilizes a generative adversarial network for segmentation to learn a mapping from seismic reflection data to lithological facies. We incorporate uncertainty analysis into the workflow using a Bayesian framework. The proposed approach accelerates the interpretation process by reducing the need for human intervention, and also lessens individual biases that an interpreter may bring. We demonstrate the effectiveness of the proposed algorithm by testing on field data examples, and show that the proposed workflow classifies facies accurately. This may potentially enable the development of depositional environment maps in areas of low well density.

INTRODUCTION

Seismic facies can be described as sedimentary units that can be distinguished from one another on the basis of different seismic characteristics such as seismic amplitude, wavelet frequency, and the geometry and continuity of reflectors (Sheriff, 1976). Analysis of seismic facies provides an effective way of gaining insight into the lithology and depositional environment, which is crucial for characterizing hydrocarbon reservoirs (Fashagba et al., 2020). Conventional seismic facies identification requires manual analysis of seismic images and gathers by interpreters. For large 3D datasets, manual interpretation of seismic facies becomes labor intensive and time consuming. In addition, manual interpretation is subjective, relying on the interpreter's experience and skill.

To improve the efficiency of conventional implementation, and reduce the manual input and subjectivity of interpretation, recent studies have proposed automating facies classification using unsupervised and supervised neural network based workflows. The unsupervised learning algorithms are able to identify facies types in a given dataset; however, correlating network output in this case with actual geological units is difficult. An additional correlation step consisting of either visualizing facies in a lower dimensional space (Gao, 2003) or using self-organized maps (Coléou et al., 2003) is required. Alternatively, supervised learning algorithms classify facies that can be interpreted directly without involving any intermediate correlation steps. Several authors have implemented different supervised-learning algorithms for seismic facies classification. Wrona et al. (2018) implemented support vector machines (SVM) using broadband 3D seismic reflection data to analyze seismic facies. Zhao (2018) and Liu et al. (2019) implemented convolutional neural network based architecture for seismic facies classification. Liu et al. (2020) proposed a semi-supervised framework for classifying lithological facies.

In this work, we propose to classify seismic facies using a deep learning framework based on a generative adversarial network for segmentation. We train the network using seismic reflection data and manually labeled facies (*true labels*) for training data. We test the network using field examples that are not a part of the training dataset and analyze the factors affecting network output, along with corresponding uncertainties.

IMPLEMENTATION OF THE PROPOSED ALGORITHM

We adopt the framework of generative adversarial networks (GANs) (Goodfellow et al., 2014) for semantic segmentation (Luc et al., 2016). We optimize the objective function by using a combination of adversarial loss and multi-class cross-entropy loss (Luc et al., 2016), as given by:

$$L = \sum_{n=1}^{N} l_{mce}(s(x_n), y_n) - \lambda (l_{bce}(a(x_n, y_n), 1) + l_{bce}(a(x_n, s(x_n)), 0)). \tag{1}$$

The first term in Equation 1 is multi-class cross-entropy (MCE) loss required for the network to predict the correct class label at each pixel location, and the second term is the adversarial loss term that drives the segmentation model to generate label maps that cannot be distinguished from ground truth. The combination of MCE and adversarial loss terms gives the total loss, which enforces a longer range of spatial label contiguity without the addition of complexity to the test model (Luc et al., 2016). Let input to the network be denoted by x and $s(x)$ be the class probability over the number of classes that are needed for classification. Let $a(x,y) \in [0,1]$ be the scalar probability of the adversarial network, predicting y to be the ground-truth label map of input x rather than the label map given by segmentation model s. Given N input training images x_n with corresponding true labels y_n, multi-cross entropy and adversarial loss training can be summarized by Equation 1 (Luc et al., 2016)

The overall network training constitutes training both the adversarial and segmentation model. The adversarial part minimizes the binary-classification loss and the segmentation model minimizes multi-class entropy loss. In practice, to update the segmentation model, we use $\lambda l_{bce}(a(x_n, s(x_n)), 1)$ instead of $-\lambda l_{bce}(a(x_n, s(x_n)), 0)$ in Equation 1 because the former formulation results in a stronger gradient in initial learning stages (Goodfellow et al., 2014) and speeds up the training process (Luc et al., 2016). We train the network using the Adam optimizer with 60 epochs and a batch size of 32.

UNCERTAINTY AND NETWORK OUTPUT

For the deployment of deep neural networks (DNN), the uncertainty quantification represents the confidence one can have

10.1190/segam2021-3583072.1

in neural network predictions. Two types of uncertainties are associated with a neural network model, aleatoric and epistemic uncertainties (Gal, 2016; Postels et al., 2019; Pham and Fomel, 2020). Aleatoric uncertainty is inherent to data and arises from noisy observations, whereas epistemic uncertainty includes uncertainty in model parameters. The latter is better at quantifying the credibility of neural network predictions (Postels et al., 2019). To compute uncertainty, we use dropout at the inference time and compute multiple predictions for each pixel. The use of dropout layers in neural networks is equivalent to Bayesian approximation (Zhu and Laptev, 2017). The key is to pass the input through the network a given number of times with random dropouts, find the mean of the prediction, and compute variance to obtain the model uncertainty.

NUMERICAL EXAMPLES

We demonstrate application of the proposed method using data from Parihaka in New Zealand provided by New Zealand Crown Minerals. The 3D volume is $1006 \times 590 \times 782$, where 590 and 782 are inlines and crosslines. The training labels for this 3D seismic volume have been provided by Chevron U.S.A. Inc. The dataset has six different facies, with each pixel in the volume assigned a value between 1 and 6. These facies differ from one another in terms of seismic amplitude, reflector geometry, and continuity as shown in Table 1. We divide the 3D volume into 2D patches of size 200×200 samples along inline and crossline directions, which results in 59,600 patches. We train the network using 27,648 patches and use the remaining patches for validation. We further test the trained network on a nearby seismic volume from the same basin consisting of 782 crosslines and 251 inlines divided into 24,560 patches.

Seismic data used for training and validation is shown in Figure 1a. The comparison between the predicted facies and the true labels is shown in Figure 1b and 1c. We extract one inline section from the validation dataset with the seismic section, predicted labels using DNN, and the true labels shown in Figure 2a, 2b, and 2c, respectively. Predicted labels are close to true labels; however, there are some areas such as the one marked by red circle in Figure 2b where the network associates change in seismic amplitudes to change in facies type. Next, we extract one of the validation crosslines. Figure 3a, 3b, and 3c shows the seismic section, predicted facies, and true facies labels, respectively. The proposed algorithm accurately classifies facies, especially slope valleys and submarine canyon systems with channels, which have lesser frequency of occurrence as compared to other facies. To further analyze the output of the proposed method, we plot the recall, precision, and F1 score for validation data in Figure 4a, 4b, and 4c. Scores indicate that facies classification using the proposed approach is close to that of the true labels; however, the precision score for the slope valley complex is lower than that of remaining facies, which is expected because of lowest frequency of occurrence of these facies.

We extend testing to another seismic volume in the Parihaka Basin. We extract one of the crosslines from the training and validation volume and the same crossline from the test volume to observe geological continuity of facies. Note the plot of the seismic section in Figure 5a with the blue outline region indicating the training and validation section and red outline indicating the test section. In the seismic, note that the facies are continuous as we move from the training to the test section, and therefore, we expect similar behavior in the predicted facies as well, which is shown in Figure 5b. We plot a crossline section from the test volume with a seismic section, predicted labels, and the corresponding uncertainty in prediction shown in Figure 6a, 6b, and 6c. The predicted facies follow the seismic events, and the uncertainty values are low except at the boundaries of the facies, which is the transition zone from one facies type to another.

Table 1: List of density, elastic properties, and fractions of rock minerals used in this study (details provided by Chevron).

Facies No	Rock type	Seismic characteristics
1	Basement rocks	Low S/N ratio
2	Slope mudstone A	High amplitude upper and lower boundaries
3	Mass transport complex	Mix of chaotic facies and low amplitude parallel reflectors
4	Slope mudstone B	High-amplitude parallel reflectors
5	Slope valley	High amplitude incised channels
6	Submarine canyon	Low amplitude mix of parallel surfaces and chaotic reflectors

CONCLUSIONS

We have introduced a deep neural network based framework to automate the seismic facies classification workflow. The output of the proposed algorithm is geologically plausible and close to the true labels. The proposed algorithm provides a robust workflow for seismic facies classification without the need for human interpretation other than that for creating training labels; hence, it improves the efficiency of conventional interpretation workflows. We incorporate uncertainty analysis in the framework to estimate the confidence level in the neural network output. Some sections like one of the validation inline sections indicate the possibility of correlation between seismic amplitudes and output of the proposed method, which warrants further investigation.

ACKNOWLEDGMENTS

We thank Dimitri Bevc, Adam Halbert, and Bruce Power from Chevron for organizing the SEG 2020 Post-Convention Workshop ”Machine Learning Blind-Test Challenge” and providing the interpretation labels used for training. We thank Jake Covault and Zoltan Sylvester for inspiring discussions.

10.1190/segam2021-3583072.1

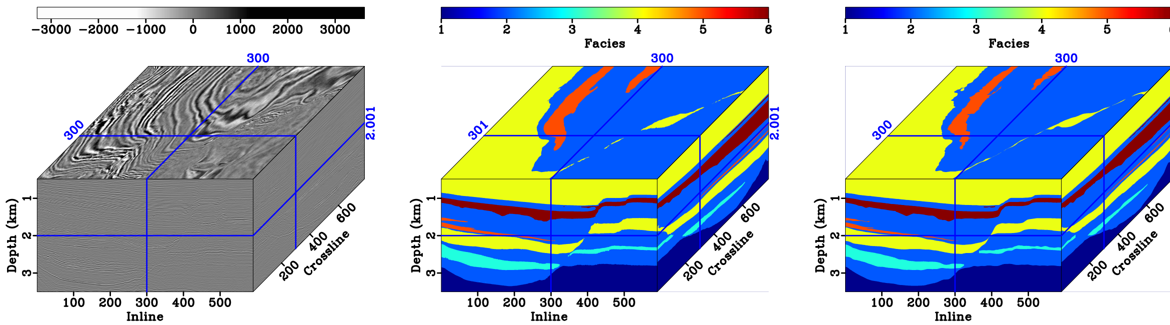

(a) (b) (c)

Figure 1: 3D data from Parihaka New Zealand: (a) 3D seismic data. (b) Predicted labels. (c) True labels.

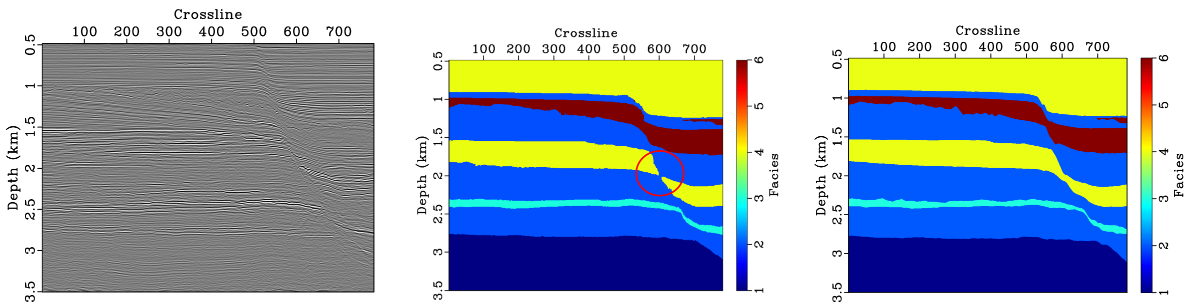

(a) (b) (c)

Figure 2: One of the validation inline sections: (a) Seismic section. (b) Predicted labels. (c) True labels.

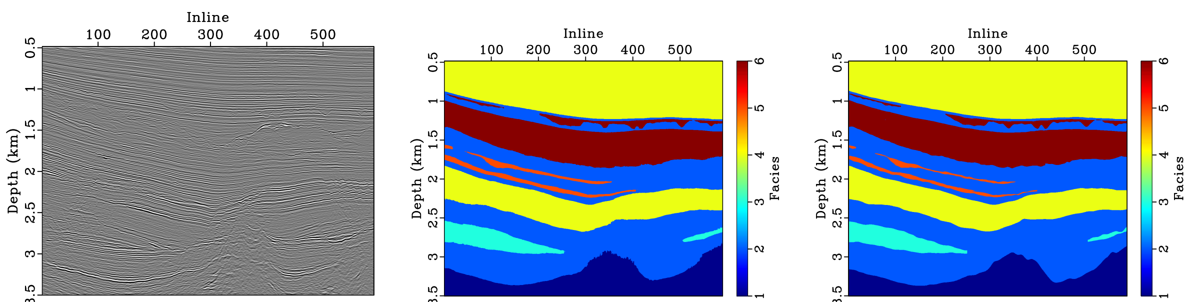

(a) (b) (c)

Figure 3: One of the validation crossline sections: (a) Seismic section. (b) Predicted labels. (c) True labels.

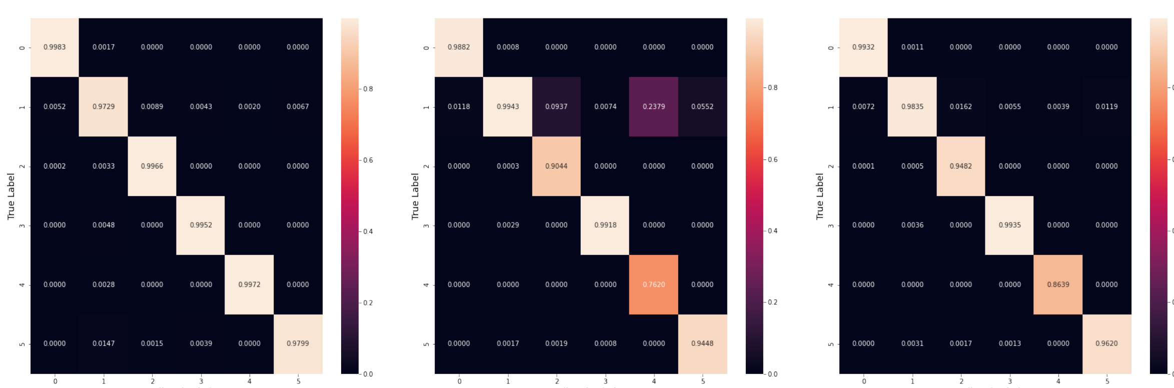

(a) (b) (c)

Figure 4: Performance metrics: (a) Recall score. (b) Precision score. (c) F1 score.

10.1190/segam2021-3583072.1

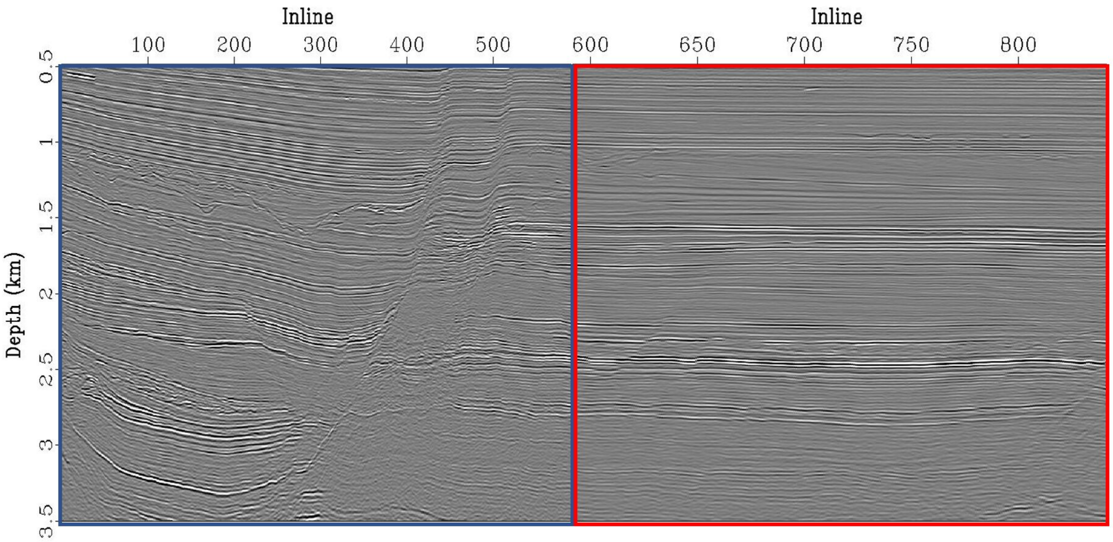

(a)

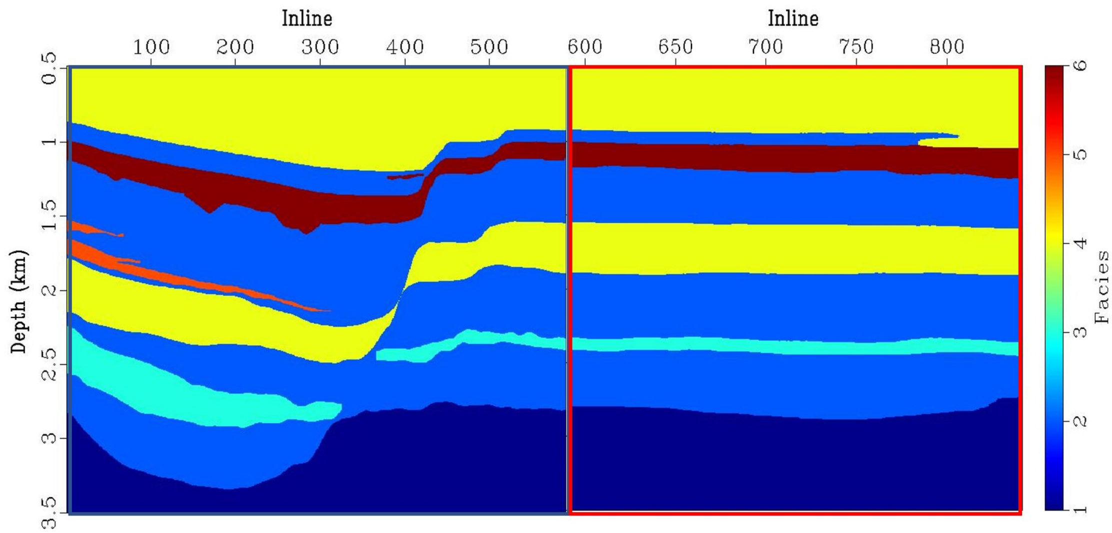

(b)

Figure 5: One of the test crossline sections extracted from training and test volume: Blue box indicates training area and red indicates test area. (a) Seismic section. (b) Facies.

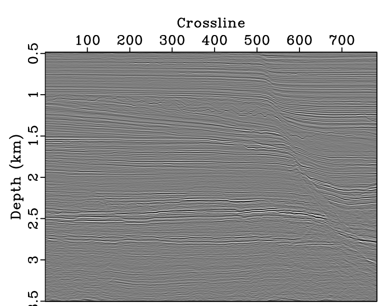

(a)

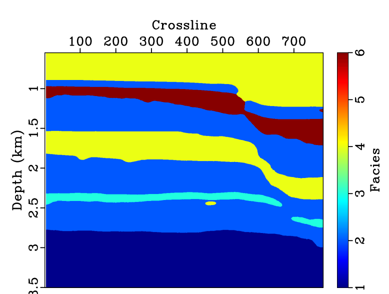

(b)

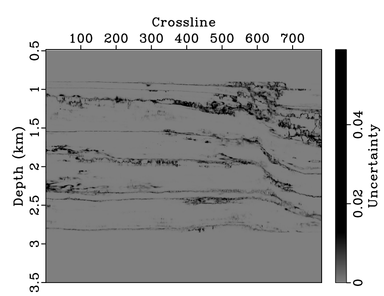

(c)

Figure 6: One of the crosslines from test volume: (a) Seismic section. (b) Predicted facies using proposed method. (c) Uncertainty in prediction using proposed method.

REFERENCES

Coléou, T., M. Poupon, and K. Azbel, 2003, Unsupervised seismic facies classification: A review and comparison of techniques and implementation: The Leading Edge, **22**, 942–953, doi: https://doi.org/10.1190/1.1623635.

Fashagba, I., P. Enikanselu, A. Lanisa, and O. Matthew, 2020, Seismic reflection pattern and attribute analysis as a tool for defining reservoir architecture in 'SABALO'field, deepwater Niger Delta: Journal of Petroleum Exploration and Production Technology, **10**, 991–1008, doi: https://doi.org/10.1007/s13202-019-00807-1.

Gal, Y., 2016, Uncertainty in deep learning: University of Cambridge, 4.

Gao, D., 2003, Volume texture extraction for 3D seismic visualization and interpretation: Geophysics, **68**, 1294–1302, doi: https://doi.org/10.1190/1.1598122.

Goodfellow, I. J., J. Pouget-Abadie, M. Mirza, B. Xu, D. Warde-Farley, S. Ozair, A. Courville, and Y. Bengio, 2014, Generative adversarial networks: arXiv preprint arXiv:1406.2661.

Liu, M., M. Jervis, W. Li, and P. Nivlet, 2020, Seismic facies classification using supervised convolutional neural networks and semisupervised generative adversarial networks: Geophysics, **85**, no. 4, O47–O58, doi: https://doi.org/10.1190/geo2019-0627.1.

Liu, Z., J. Cao, Y. Lu, S. Chen, and J. Liu, 2019, A seismic facies classification method based on the convolutional neural network and the probabilistic framework for seismic attributes and spatial classification: Interpretation, **7**, no. 3, SE225–SE236, doi: https://doi.org/10.1190/INT-2018-0238.1.

Luc, P., C. Couprie, S. Chintala, and J. Verbeek, 2016, Semantic segmentation using adversarial networks: arXiv preprint arXiv:1611.08408.

Pham, N., and S. Fomel, 2020, Uncertainty estimation using Bayesian convolutional neural network for automatic channel detection: SEG Technical Program, Expanded Abstracts, 3462–3466, doi: https://doi.org/10.1190/segam2020-3427239.1.

Postels, J., F. Ferroni, H. Coskun, N. Navab, and F. Tombari, 2019, Sampling-free epistemic uncertainty estimation using approximated variance propagation: Proceedings of the IEEE/CVF International Conference on Computer Vision, 2931–2940.

Sheriff, R., 1976, Inferring stratigraphy from seismic data: AAPG Bulletin, **60**, 528–542, doi: https://doi.org/10.1306/83D923F7-16C7-11D7-8645000102C1865D.

Wrona, T., I. Pan, R. L. Gawthorpe, and H. Fossen, 2018, Seismic facies analysis using machine learning: Geophysics, **83**, no. 5, O83–O95, doi: https://doi.org/10.1190/geo2017-0595.1.

Zhao, T., 2018, Seismic facies classification using different deep convolutional neural networks: SEG Technical Program, Expanded Abstracts, 2046–2050, doi: https://doi.org/10.1190/segam2018-2997085.1.

Zhu, L., and N. Laptev, 2017, Deep and confident prediction for time series at Uber: 2017 IEEE International Conference on Data Mining Workshops (ICDMW), 103–110.

10.1190/segam2021-3583072.1